Submitted to Physics Letters B

LBL-1020 Rev.
Preprint

STRUCTURE IN THE $2\pi^0$ MASS SPECTRUM IN THE REACTION $\pi^- p \to n\pi^0\pi^0$ AT 1.6 TO 2.4 GeV/c

A. Skuja, M. A. Wahlig, T. B. Risser, M. Pripstein,
J. E. Nelson, I. R. Linscott, R. W. Kenney, O. I. Dahl,
and R. B. Chaffee

March 1973

Prepared for the U.S. Atomic Energy Commission
under Contract W-7405-ENG-48

DISCLAIMER

STRUCTURE IN THE $2\pi^0$ MASS SPECTRUM IN THE REACTION $\pi^- p \to n\pi^0\pi^0$ AT 1.6 TO 2.4 GeV/c*

A. Skuja,** M. A. Wahlig, T. B. Risser,*** M. Pripstein, J. E. Nelson, I. R. Linscott,† R. W. Kenney, O. I. Dahl, and R. B. Chaffee‡

Lawrence Berkeley Laboratory, University of California
Berkeley, California 94720

March 1973

ABSTRACT

We report results from a study of the reaction $\pi^- p \to n\pi^0\pi^0$ between 1.6 and 2.4 GeV/c, in which all the final-state particles were detected with a 3.7 π steradian array of optical spark chambers and shower counters, and neutron counters subtending a polar lab angle region of 12 to 72 degrees. The $2\pi^0$ mass spectrum exhibits a marked enhancement in the region of 800 MeV. In terms of I = 0, S-wave π-π phase shifts, the data are consistent with the recently reported "Down-Down" solution above 800 MeV but are in disagreement below that dipion mass.

---

* Work done under the auspices of the U. S. Atomic Energy Commission.

** Present address: Nuclear Physics Laboratory, Oxford, University, Keble Road, Oxford, England.

*** Present address: University of California at Santa Barbara, Santa Barbara, California 93106.

† Present address: Syracuse University, Syracuse, N.Y. 13210

‡ Present address: Stanford Linear Accelerator Center, Stanford University, Stanford, California 94305

The properties of the scalar dipion system (isotopic spin I = 0, angular momentum J = 0) have been the subject of much controversy [1] since the discovery of the persistent "forward-backward" asymmetry in the decay of the peripherally produced neutral $\rho(765)$ meson. Most of the information has come from studies of the π^+-π^- system in which the analyses have been complicated by the dominant ρ production. A more sensitive approach is to study the reaction

$$\pi^- + p \to n + \pi^0 + \pi^0, \qquad (1)$$

in which ρ production is forbidden. Although the dipion system in reaction (1) can have I = 2 as well as I = 0, previous studies indicate that there is no structure in the I = 2 dipion system [2]; thus, any structure in the $2\pi^0$ system may be attributed to the I = 0 state.

We have performed an experiment at the Berkeley Bevatron to study reaction (1) at beam momenta of 1.59 to 2.39 GeV/c in 0.20 GeV/c intervals. The salient features of the experiment are 1) a very high probability for detecting γ-rays and 2) identification of the final state by detecting the neutron and all the γ-rays from the π^0-decays. The kinematic variables of each of the particles were measured, and an over-constrained (6-constraint, 3-vertex) kinematic fit was made to each event using a modified version of the LBL Group A bubble chamber program SQUAW [3].

A schematic diagram of the experimental layout is shown in Fig. 1. A detailed description of all the apparatus and its performance characteristics is given in refs. [4-6]. The π^- beam from the Bevatron had a momentum bite of $\pm 1\%$, and was focused to a spot size of 1.5 in. horizontally by 0.75 in. vertically (FWHM) at a liquid hydrogen

target, 8 in. long by 4 in. in diameter. Counter hodoscopes defined the beam direction at the target to within ±0.2 deg (rms). The target was surrounded by anti-coincidence counters which vetoed any interaction in which charged particles were produced. A neutral-final-state trigger was defined by a coincidence of a 3-counter beam telescope and no signal from the anti-counters. The beam contamination of μ^- and e^- was monitored by a threshold Cerenkov counter. The γ-rays were detected by a large cubic array of lead-plate optical spark chambers [4-6] surrounding the target and covering five sides of a cube, with the sixth side (beam entrance face) almost completely covered by shower counters of lead-scintillator sandwiches (G_i in fig. 1). The lab solid angle subtended for γ-ray detection was 3.7 π steradians. Each of the four side chambers was about 7 radiation lengths thick, and the downstream chamber was about 8 radiation lengths thick. The chamber plates were made very thin (1/32 in. lead sandwiched between two sheets of 1/64 in. aluminum) in order to ensure a high detection efficiency for low energy showers [7]. The first four gaps in each chamber had aluminum plates 3/64 in. thick and were used as a visual aid to identify any charged particles which managed to enter the chambers. Each chamber was photographed in two orthogonal views for 90 deg stereo.

The neutron detector consisted of 20 cylindrical plastic scintillation counters, each 8 in. in diameter and 8 in. long, located about 15 ft from the target (as shown in fig. 1) and subtending polar lab angles (θ_n) from 12 to 72 deg with respect to the central beam ray. Each neutron counter had an additional counter mounted in front of it to veto charged particles. The timing gate for the neutron detector

was set to accept neutrons of velocity (β) in the region $0.17 \leq \beta \leq 0.84$ [8]. The neutron counter timing resolution was ±0.6 ns [4, 5].

Data were collected in two different modes of electronic triggering conditions: 1) a neutron counter signal in coincidence with a neutral-final-state trigger as described above and 2) a neutral-final-state trigger only [9]. Systematic biases (e.g. neutron scattering in the chambers) were checked by comparing the differential cross sections for the 2-body final states, $n\pi^0$ and $n\eta$, as measured in the two triggering modes. The neutral-final-state trigger data were also used to determine partial cross sections for the various neutral final states, as described in ref. [6]. Cross sections for reaction (1) are listed in table 1.

The film was examined by a group of scanners who recorded the number of showers and the location of the first spark of each shower. The film was then measured and digitized on the LBL SASS machine [10] —a precision cathode ray tube and photomultiplier system linked to a DDP-24 computer. This information was processed by a pattern-recognition program which reconstructed the shower geometry in three-dimensional space using the scanner's shower information as a guide. These data, together with the counter information, were then subjected to a kinematic fit using the LBL program SQUAW [3]. The γ-ray energy measurement from spark counting was calibrated by an overconstrained kinematic fit of the 2-shower events to $n\pi^0$ and $n\eta$ final states [11].

The study of the dynamical properties of reaction (1) was made with the neutron-trigger data sample containing four visible showers in the chambers and no upstream shower-counter signal. The data sample consists of about 7400 events within our timing gate [corresponding

to invariant four-momentum transfers to the nucleon ($-t_{p\to n}$) of 0.029 to 1.54 $(GeV/c)^2$] that fit reaction (1) with χ^2 probability $\geq 5\%$ [12]. The $2\pi^0$ mass resolution is approximately ±35 MeV (HWHM) over most of the mass region. The data within the neutron counter acceptance region in t and θ_n have been corrected for neutron scattering in the chambers, neutron counter geometry, and detection efficiency [4]. The average weight per event is ~1.7. Structure is evident in both the $n\pi^0$ and $\pi^0\pi^0$ mass plots. The dominant feature, at all values of t, is the $n\pi^0$ spectrum (not shown) corresponding to $\Delta^0(1236)$ production [13]. In order to study the properties of the $2\pi^0$ system, free from the effects due to Δ(1236), we cut out all events having at least one $n\pi^0$ combination in the broad mass band of 1100 to 1300 MeV. The $n\pi^0$ mass spectrum of the surviving events exhibits no resonant structure.

Figure 2 displays the combined data from the five beam momenta, with the Δ-band events excluded. The t-distribution (fig. 2a) is characterized by a pronounced peak at low t. The curve shown represents the prediction of "peripheral phase-space" (PPS) for the region $-t \leq 0.3\ (GeV/c)^2$. This t-cut henceforth specifies the peripheral region. PPS is defined as [(phase-space)$\cdot(-t)/(t-\mu^2)^2\cdot F(t)$], where μ is the pion mass and F(t) is the Dürr-Pilkuhn vertex factor [14] multiplied by Wolf's t-dependent form factor [15]:

$$F(t) = \frac{(2.3-\mu^2)^2}{(2.3-t)^2}\cdot\frac{(1+2.66^2 q_n^2)}{(1+2.66^2 q_t^2)}. \qquad (2)$$

q_t is the momentum of the incoming target proton evaluated in the neutron rest frame and q_n is this quantity evaluated with $t = \mu^2$. This PPS distribution fits the peripheral t-distribution very well, as shown by the curve in fig. 2(a) normalized to the data below 1 GeV dipion

mass (solid histogram).

Figure 2(b) shows the $2\pi^0$ mass spectrum (1323 events) for events in the peripheral region. The curve represents the PPS distribution normalized to the data below 1000 MeV but excluding the 700 to 900 MeV region. The mass spectrum exhibits a marked enhancement in the 800 MeV region. This pronounced structure is also evident in the mass spectrum for the entire t region (4088 events) shown in fig. 2(c). Although the background here is greater and of a different shape than the background in the peripheral region, the same enhancement in the mass spectrum is clearly evident. The curve represents a crude approximation of the spectrum as the sum of phase-space and PPS, the relative amounts being determined by a fit to the t-distribution at each momentum.

In accordance with our introductory remarks, the observed structure may be attributed to an I = 0 π-π interaction. To determine the angular momentum (J) we studied the dipion decay angular distribution with respect to the incident π^- direction in the dipion rest frame, for events in the peripheral region. For all $2\pi^0$ masses below about 940 MeV, the decay distribution was consistent with isotropy outside the region corresponding to the Δ-mass-band cut and hence is consistent with J = 0 for the dipion system.

To parametrize the peripheral data we assume the one-pion exchange (OPE) mechanism as a production model, using the Chew-Low equation [16] modified by the form factor F(t) defined above, and work in the physical region (since there are too few events to make a meaningful extrapolation to the pion pole). Cross sections for this t-cut were determined by normalizing the neutron-counter data to the neutral-final-state-trigger cross sections (table 1), as out-

lined in ref. [4], and are listed in table 1 [17]. The formula used, relating the "off-shell" cross section, $d^2\sigma/dm_{\pi\pi}dt$, to the "on-shell" cross section $\sigma_{\pi\pi}$, in the S-wave approximation, is

$$d^2\sigma/dm_{\pi\pi}\,dt = \frac{1}{4\pi M^2 P_L^{\,2}} \frac{|t|}{(t-\mu^2)^2} \frac{g^2}{4\pi} m_{\pi\pi}^2\, q\, \sigma_{\pi\pi} \cdot F(t), \qquad (3a)$$

$$\sigma_{\pi\pi} = \frac{4\pi}{q^2} \frac{2}{9} \sin^2(\delta_0^0 - \delta_0^2). \qquad (3b)$$

M is the proton mass, P_L is the lab beam momentum, $g^2/4\pi = 29.2$, $m_{\pi\pi}$ is the dipion mass, δ_0^0 (δ_0^2) is the I = 0 (I=2) S-wave phase shift and q is the on-shell pion momentum in the dipion rest frame [18]. To determine $\sin^2(\delta_0^0 - \delta_0^2)$, we used the following procedure which avoids possible binning problems in t and yields results which are relatively insensitive to the range of t-values chosen [19]. We perform a transformation of variables [20], mapping the t-axis onto the axis of another variable, x = x(t), such that the distribution of events (i.e., $d\sigma/dx$) is approximately uniform with respect to x. A simple choice for the transformation is of the form $dx/dt = (\mu^2 - t)^{-k}$ with k = 2 providing a sufficiently uniform distribution. Eq. (3) is then of the form $d^2\sigma/dm_{\pi\pi}dx = R(x, m_{\pi\pi}) \sin^2(\delta_0^0 - \delta_0^2)$ where $R(x; m_{\pi\pi})$ is now much more nearly constant than is the right-hand side of eq. (3a). From this expression we evaluated $\sin^2(\delta_0^0 - \delta_0^2)$ as a function of $m_{\pi\pi}$ for each beam momentum, using the procedure of ref. [4]. A weighted average of $\sin^2(\delta_0^0 - \delta_0^2)$ from all the five beam momenta is plotted as a function of $m_{\pi\pi}$ in fig. 3. The error bars in each bin are purely statistical and do not include a systematic uncertainty in the overall normalization (within ± 6 %) from our $n\pi^0\pi^0$ cross-section determination for $-t \leq 0.3$ $(GeV/c)^2$. This uncertainty is a multiplicative factor and does not affect the shape of the spectrum. The analysis does not extend beyond dipion mass of 940 MeV because of the probable presence of D-wave contribution, the amount of which is difficult to determine due to the $\Delta(1236)$ cut.

These phase-shift results are derived from our assumption of a particular OPE production model to describe our data. Although we cannot conclusively prove the validity of this description, it is nonetheless suggestive to note that the data and results are consistent with the predictions of the model, namely, i) the t-distribution of the peripheral data agrees with the model (fig. 2a), and ii) the maximum value of $\sin^2(\delta_0^0 - \delta_0^2)$, which is not constrained in the analysis, is consistent with being equal to or less than unity (fig. 3).

For purposes of comparison, we also show in fig. 3 the two phaseshift solutions at the K-mass obtained by Sarker [21] from an analysis of $K \to 2\pi$ decays. While neither solution is ruled out, our data favor Sarker's lower value. In addition, we have plotted in fig. 3 the recent phase-shift results of Protopopescu et al. [22] from an analysis of the $\pi^+ - \pi^-$ system. It is evident that the so-called "Down-Up" solution (essentially the same as that of ref. [20]) above the ρ mass is clearly in disagreement with the data and can be ruled out completely – a conclusion consistent with that of ref. [22]. Within the normalization uncertainty, the "Down-Down" solution agrees quite well with our results for $M_{\pi^0\pi^0} \geq 800$ MeV but does not agree with the results below 800 MeV. Finally, we show the theoretical predictions (curves II and III) by Basdevant et al. [23] for the phase shifts just above threshold. The curves are their solutions II and III, respectively. Neither solution can be ruled out by our results.

We wish to thank Dr. S. Parker and Dr. C. Rey for their efforts in building the excellent spark chambers, and the Bevatron crew for providing smooth beam conditions. We also thank M. Long, T. Daly, B. Hogrefe, E. Epstein and the group of scanners for their tireless efforts, and Dr. S. Protopopescu, Dr. T. Lasinski and Dr. E. Colton for fruitful discussions about π-π scattering.

Footnotes and References

1. For a review of the I = 0, J = 0 π-π system, refer to:
a) M. Derrick, Proc. of the Boulder Conference on High Energy Physics (1969) p. 291; D. Morgan and J. Pisut, Springer Tracts in Modern Physics 55 (1970) 1; J. L. Petersen, Physics Report 2C, (1971) 157.
2. E. Colton et al. Phys. Rev. D 3, 2028 (1971).
3. O. I. Dahl et al. Lawrence Berkeley Laboratory Group A Programming Note No. P-126 (unpublished).
4. A. Skuja (Ph.D. thesis), Lawrence Berkeley Laboratory Report LBL-378 (1972) (unpublished).
5. T. B. Risser (Ph.D. thesis), Lawrence Berkeley Laboratory Report UCRL-20039 (1970) (unpublished).
6. J. E. Nelson (Ph.D. thesis), Lawrence Berkeley Laboratory Report LBL-1019 (1972) (unpublished).
7. γ-ray detection threshold was about 10 MeV and the average detection probability was 89% per γ-ray, averaged over all γ-ray energies and production lab angles in multi-π^0 final states.
8. "Early-time" triggers (i.e., for time of-flight corresponding to unphysical $\beta > 1.2$) were also accepted in order to study the room background, which was small.
9. The target-empty trigger rate varied between 11 and 16% of the target-full rate, but the target-empty background was reduced to a negligible level in the neutron-trigger data after kinematic fitting to reaction (1).
10. A. R. Clark and L. T. Kerth, Proc. of the 1966 Conference on Instrumentation for High Energy Physics, Stanford, California (1966) p. 355.

11. For $E_\gamma < 300$ MeV, the γ-ray energy resolution was about ±40% and became progressively worse to nearly ±100% at $E_\gamma \approx 1$ GeV.

12. This kinematic selection criterion rejects almost all "bad" trigger events caused by neutron inelastic scattering in the spark chambers. Also, this selection, together with low feed-down and small $3\pi^0$ cross sections, results in negligible contamination of $3\pi^0$ events in our $2\pi^0$ sample.

13. For $-t < 0.3$ $(GeV/c)^2$, about 40% of the events correspond to $\Delta(1236)$ production.

14. H. P. Dürr and H. Pilkuhn, Nuovo Cimento 40 (1965) 899.

15. G. Wolf, Phys. Rev. 182 (1969) 1538.

16. G. F. Chew and F. E. Low, Phys. Rev. 113 (1959) 1640.

17. A study of the resolution of the data in both triggering modes indicates that this procedure yields the correct neutron-counter-triggered cross sections to within an uncertainty of ± 6 %.

18. In the determination of $\sin^2(\delta_0^0 - \delta_0^2)$ in ref. 4, a different form factor was used. Also, the off-shell pion momentum was used instead of the on-shell value, causing $\sin^2(\delta_0^0 - \delta_0^2)$ to be reduced by about 30%.

19. Preliminary results reported at the 1972 Batavia Conference represented only an average value of $\sin^2(\delta_0^0 - \delta_0^2)$ over the entire t-range. These values were strongly influenced by small background at high t and hence were sensitive to the t-cut used and therefore should be distrusted.

20. A different transformation of variables used by J. P. Baton et al., Phys. Letters 33B (1970) 528, appears to have a similar physical effect in that the distribution of events is more uniform in the mapped variable; as a result, better use is made of the

available statistics over a broader t-interval.

21. A. Q. Sarker, Phys. Letters 41B (1972) 157.

22. S. D. Protopopescu et al. Lawrence Berkeley Laboratory Report LBL-970 (1972), to be published in Phys. Rev. The "Down-Down" solution is their case 1 solution. The "Down-Up" solution was obtained from S. D. Protopopescu, private communication.

23. J. L. Basdevant, C. D. Froggatt, and J. L. Petersen, Physics Letters 41B (1972) 178.

Table 1. Cross sections.

P_{π^-}	$\sigma(\pi^- p \to n\pi^0\pi^0)$	$\sigma(\pi^- p \to n\pi^0\pi^0)$ for $\lvert t_{min}\rvert \leq -t \leq 0.3$ (GeV/c)^2. (a)	
		With Δ-band-cut	With Δ-band-cut corrected for (b)
(GeV/c)	(μb)	(μb)	(μb)
1.59	1310±100	180±15	325±30
1.79	1360±100	270±20	430±30
1.99	1390±90	225±20	335±30
2.19	1380±90	220±20	320±30
2.39	1140±70	165±10	225±15

(a) $\lvert t_{min}\rvert$ is determined by neutron counter acceptance in $\lvert t\rvert$ [≥ 0.029 (GeV/c)^2] and θ_n [≥ 12 deg].

(b) Correction is just ratio of phase space with and without Δ-bands removed.

Figure Captions

Fig. 1. Layout of the apparatus: (a) arrangement of spark chambers, hydrogen target and γ-ray detection counters (G_i); (b) plan view (reduced scale) of entire layout. M_i represent beam telescope counters and A_i are charged-particle anti-counters.

Fig. 2. Data within the neutron counter acceptance region in t and θ_n, and with Δ(1236) mass-band events excluded (see text): (a), t-distribution. The dotted histogram includes all data and the solid histogram includes the data for $M_{\pi^0\pi^0} < 1000$ MeV. The curve represents peripheral phase space (PPS) for $M_{\pi^0\pi^0} < 1000$ MeV, normalized to the data in the solid histogram for $-t \leq 0.3$ (GeV/c)^2; (b)-(c), $2\pi^0$ mass spectrum for the t region indicated. The curve in (b) represents PPS while that in (c) represents a combination of phase space and PPS (see text). Both curves are normalized to the corresponding data below 1000 MeV but outside the 700-900 MeV region.

Fig. 3. Phase-shift results. $\sin^2(\delta_0^0 - \delta_0^2)$ as a function of $M_{\pi^0\pi^0}$. The solid (dashed) curve above 550 MeV corresponds to the "Down-Down" ("Down-Up") solution from Protopopescu et al. [22]. Curves II and III are solutions II and III, respectively, from Basdevant et al. [23]. The corresponding S-wave scattering lengths (a_s^I), in units of m_π^{-1} are $a_s^0 = 0.16$ and $a_s^2 = -0.048$ for solution II and $a_s^0 = 0.60$ and $a_s^2 = 0.043$ for solution III. The dashed points at the K-mass are from Sarker [21].

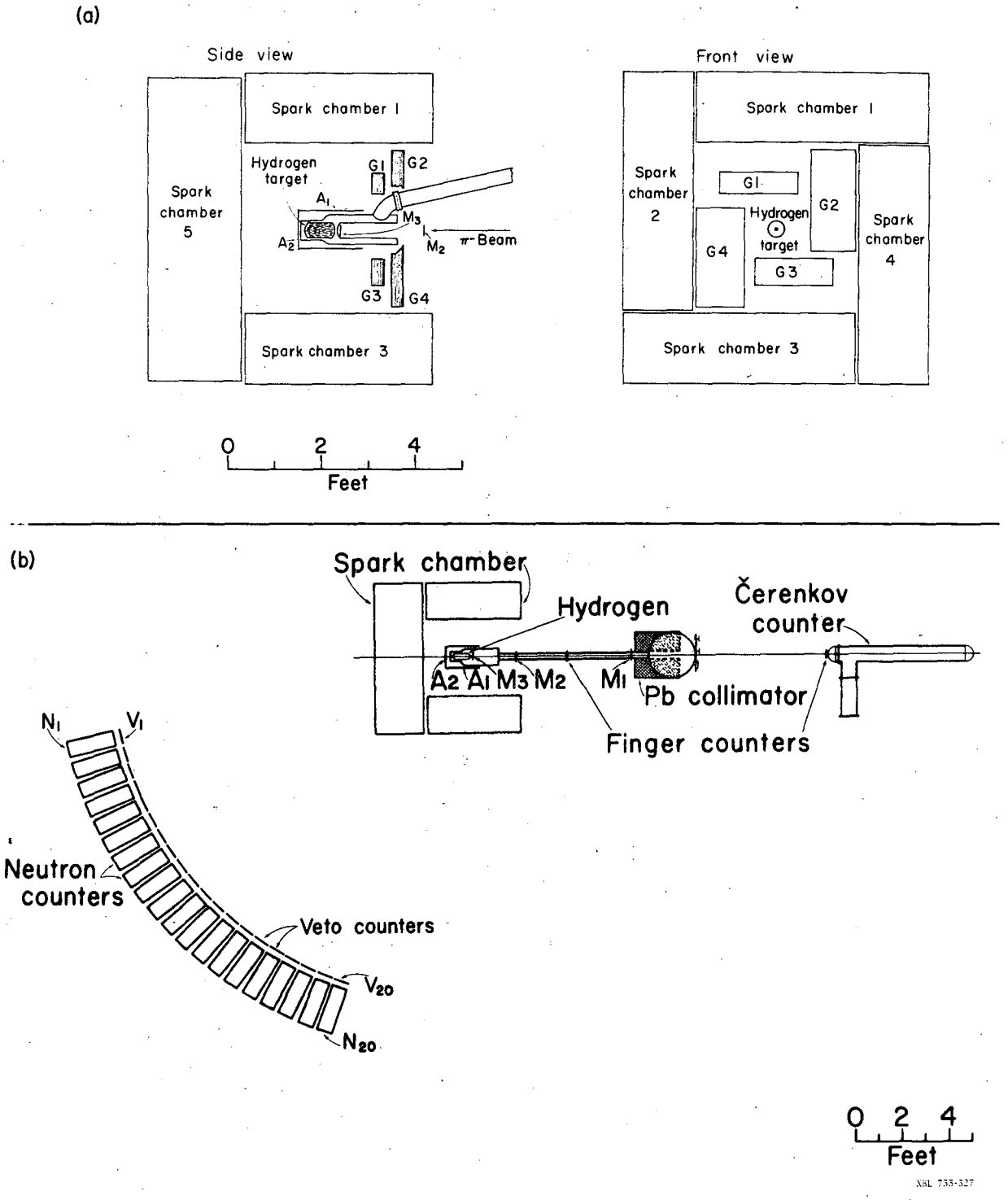
(a)
Side view
Spark chamber 1
Spark chamber 5
Hydrogen target
G1
G2
A1
A2
M3
M2
π⁻Beam
G3
G4
Spark chamber 3
Front view
Spark chamber 1
Spark chamber 2
G1
G2
G4
Hydrogen target
G3
Spark chamber 4
Spark chamber 3
0 2 4
Feet
(b)
Spark chamber
Hydrogen
Čerenkov counter
A2 A1 M3 M2
M1
Pb collimator
Finger counters
N1
V1
Neutron counters
Veto counters
V20
N20
0 2 4
Feet
XBL 733-327

Fig. 1

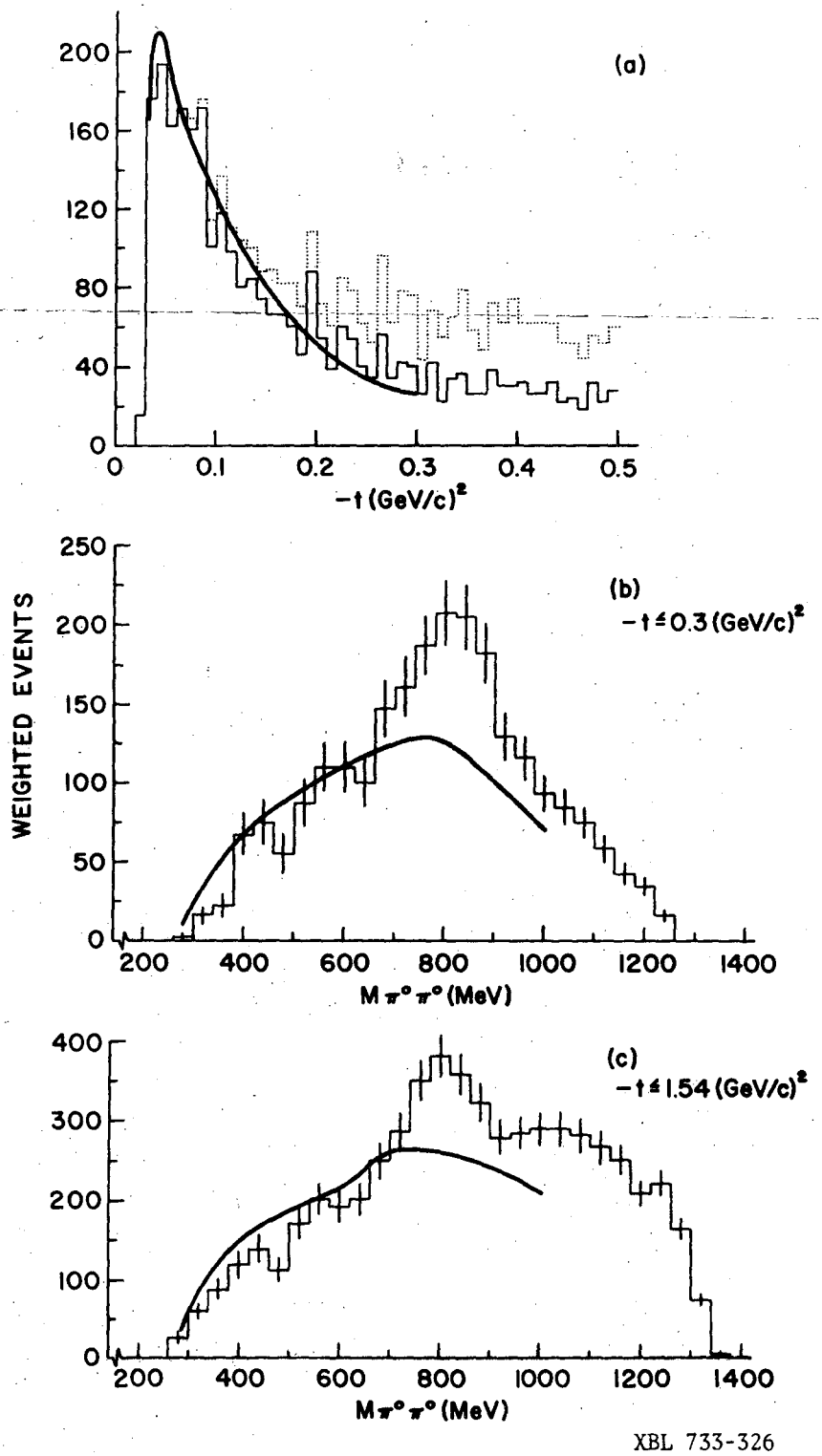
(a)
200
160
120
80
40
0
0
0.1
0.2
0.3
0.4
0.5
−t (GeV/c)²
(b)
−t ≤ 0.3 (GeV/c)²
WEIGHTED EVENTS
250
200
150
100
50
0
200
400
600
800
1000
1200
1400
M π° π° (MeV)
(c)
−t ≤ 1.54 (GeV/c)²
400
300
200
100
0
200
400
600
800
1000
1200
1400
M π° π° (MeV)
XBL 733-326

Fig. 2

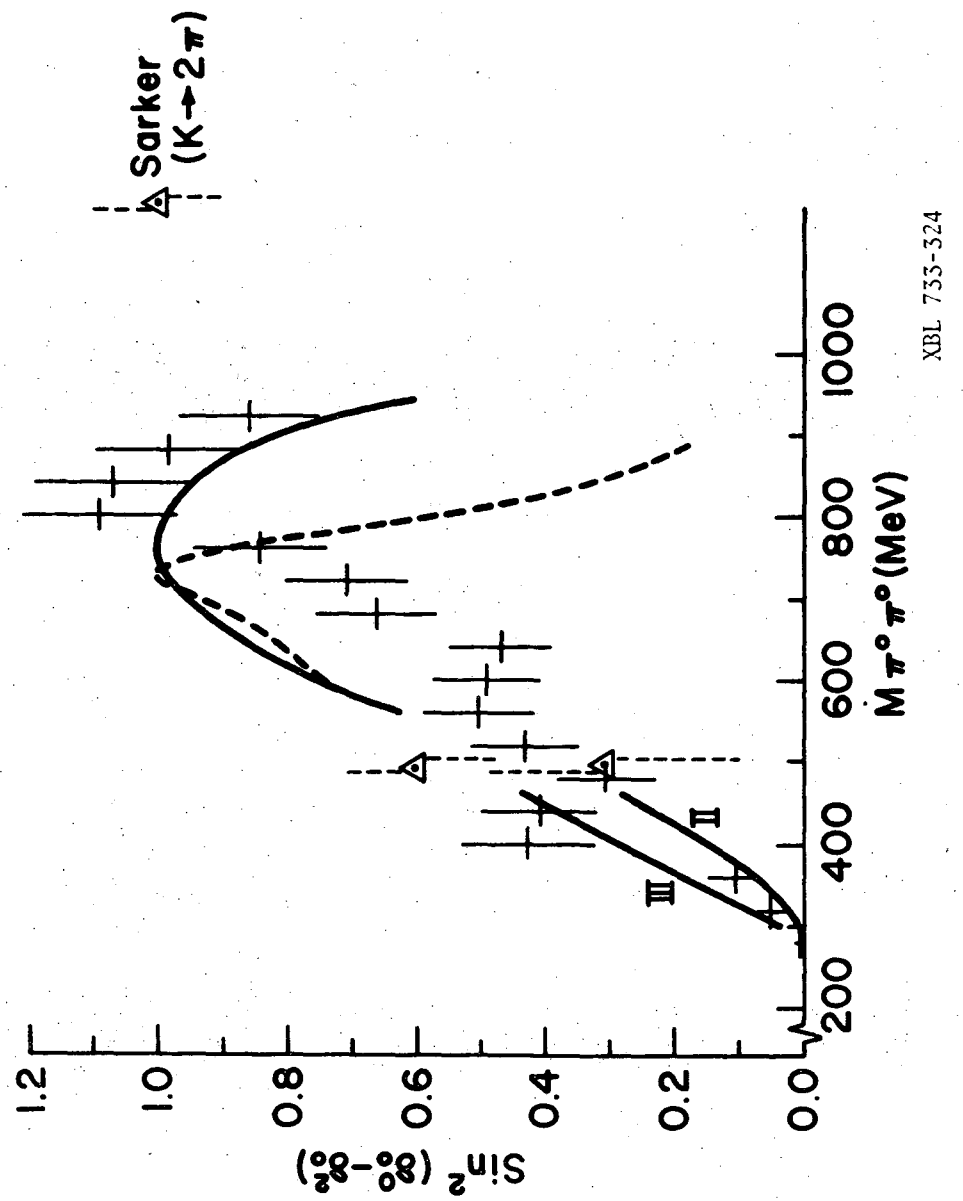

XBL 733-324

Fig. 3

TECHNICAL INFORMATION DIVISION
LAWRENCE BERKELEY LABORATORY
UNIVERSITY OF CALIFORNIA
BERKELEY, CALIFORNIA 94720